Biochimica et Biophysica Acta 1808 (2011) 649–655

Contents lists available at ScienceDirect

Biochimica et Biophysica Acta

journal homepage: www.elsevier.com/locate/bbamem

Interaction of cationic bilayer fragments with a model oligonucleotide

Julio H.K. Rozenfeld [a], Tiago R. Oliveira [b], M. Teresa Lamy [b], Ana M. Carmona-Ribeiro [a,*]

[a] Departamento de Bioquímica, Instituto de Química, Universidade de São Paulo, CP 26077, CEP 05513-970, São Paulo,SP, Brazil
[b] Departamento de Física Geral, Instituto de Física, Universidade de São Paulo, CP 66318, CEP 05315-970, São Paulo,SP, Brazil

ARTICLE INFO

Article history:
Received 15 October 2010
Received in revised form 26 November 2010
Accepted 30 November 2010
Available online 11 December 2010

Keywords:
Dioctadecyldimethylammonium bromide
3′-AAA AAA AAA A-5′ oligonucleotide
2′-deoxyadenosine-5′-monophosphate
Differential scanning calorimetry
Dynamic light scattering
Fusion of bilayer fragments

ABSTRACT

The interaction between cationic bilayer fragments and a model oligonucleotide was investigated by differential scanning calorimetry, turbidimetry, determination of excimer to monomer ratio of 2-(10-(1-pyrene)-decanoyl)-phosphatidyl-choline in bilayer fragment dispersions and dynamic light scattering for sizing and zeta-potential analysis. Salt (Na_2HPO_4), mononucleotide (2′-deoxyadenosine-5′-monophosphate) or poly (dA) oligonucleotide (3′-AAA AAA AAA A-5′) affected structure and stability of dioctadecyldimethylammonium bromide bilayer fragments. Oligonucleotide and salt increased bilayer packing due to bilayer fragment fusion. Mononucleotide did not reduce colloid stability or did not cause bilayer fragment fusion. Charge neutralization of bilayer fragments by poly (dA) at 1:10 poly (dA):dioctadecyldimethylammonium bromide molar ratio caused extensive aggregation, maximal size and zero of zeta-potential for the assemblies. Above charge neutralization, assemblies recovered colloid stability due to charge overcompensation. For bilayer fragments/poly (dA), the nonmonotonic behavior of colloid stability as a function of poly (dA) concentration was unique for the oligonucleotide and was not observed for Na_2HPO_4 or 2′-deoxyadenosine-5′-monophosphate. For the first time, such interactions between cationic bilayer fragments and mono- or oligonucleotide were described in the literature. Bilayer fragments/oligonucleotide assemblies may find interesting applications in drug delivery.

1. Introduction

The cationic lipid dioctadecyldimethylammonium bromide (DODAB) can be dispersed in aqueous solution by several methods yielding useful bilayers [1]. Sonication of DODAB powder in water with a high energy input not only produced bilayer vesicles but also disrupted them, thereby generating open and small bilayer fragments (BF) [2]. The main evidences for the existence of BF in the sonicated dispersions were (1) osmotic nonresponsiveness suggesting absence of inner vesicle compartment [1,3], (2) direct visualization by transmission electron microscopy (TEM) [4] or cryo-TEM microscopy [5,6] (3) quasi-elastic light scattering and electron paramagnetic resonance spectroscopy data [7,8] and (4) coexistence of fluid and solid bilayer phases [9]. The size, charge and hydrophobic features of DODAB BF led to novel applications in solubilization of hydrophobic drugs [10–12], production of biomimetic particles from bilayer coverage of silica [13] or polystyrene particles [14] and design of vaccines [15,16]. However, BF applications in DNA or oligonucleotide delivery still remain poorly explored.

Antisense oligonucleotides are small single-stranded DNA molecules designed to specifically hybridize a messenger RNA inside a cell and inhibit the expression of proteins corresponding to this messenger [17]. Since the demonstration that synthetic oligonucleotides could inhibit the replication of the Rous sarcoma virus [18], antisense oligonucleotides have been considered a great promise as therapeutic agents. Nowadays, several oligonucleotide-based formulations have reached the clinical trial phase [19,20]. Antisense oligonucleotides have also been extensively used in basic research on gene expression and function [21–23], vaccine design [24], allergy [25] and cancer therapy [26]. In all cases, several obstacles must still be overcome such as degradation of oligonucleotides by nucleases on the extracellular milieu or inside the endosome and poor capture by the target cells [23,27]. Hence, suitable carriers able to protect oligonucleotides in the biological milieu are paramount for effective delivery [23,26–28].

In this work, interactions between a model oligonucleotide poly (dA) and DODAB BF are described for the first time. Major effects of inorganic phosphate salt, nucleotide or oligonucleotide on structure and colloid stability of BF are described by means of calorimetry, turbidimetry, fluorescence and dynamic light scattering for sizing and zeta-potential analysis. Oligonucleotide and salt increased bilayer packing due to BF fusion. Colloid instability induced by oligonucleotide or salt could be associated with bilayer fusion. In contrast, mononucleotide did not reduce colloid stability over the low range of concentrations tested and did not cause BF fusion.

* Corresponding author. Tel.: +55 11 3091 2164; fax: +55 11 3815 5579.
E-mail address: mcribeir@iq.usp.br (A.M. Carmona-Ribeiro).

0005-2736/$ – see front matter © 2010 Elsevier B.V. All rights reserved.
doi:10.1016/j.bbamem.2010.11.036

2. Material and methods

2.1. Materials

Dioctadecyldimethylammonium bromide (DODAB) 99.9% pure and 2′-deoxyadenosine-5′-monophosphate (dAMP) were purchased from Sigma Chemical Co. (St. Louis, MO, USA). Sodium monohydrogen phosphate (Na_2HPO_4) was purchased from Merck (RJ, Brazil). Ten-base single-stranded oligonucleotide 3′-AAA AAA AAA A-5′ (poly (dA)) was purchased from Integrated DNA Technologies IDT (Coralville, IA, USA) and stock solution was prepared in sterile Milli-Q water. 2-(10-(1-pyrene)-decanoyl)-phosphatidyl-choline (PyPC) was supplied by Molecular Probes (Eugene, OR, USA). Ultrapure water of Milli-Q-Plus quality was used throughout. For 0.5–2.5 mM Na_2HPO_4 or dAMP solutions in water, the pH measured was constant for 40 minutes and equal to 8.0 and 3.5, respectively. This showed that the first electrolyte can be considered divalent and the second, monovalent.

2.2. Preparation of DODAB dispersions

Bilayer fragments (BF) were produced by 20 minutes sonication of the DODAB powder in water with a macrotip connected to a Fischer Scientific 550 Sonic Dismembrator set to 25% of its maximum power [3]. Thereafter, centrifugation (1 h/10,000*g*) removed titanium particles released from the macrotip [29]. DODAB concentration was analytically determined by halide microtitration [30].

DODAB large unilamellar vesicles (LV) were obtained by vortexing the lipid powder in water solution at 60 °C [31]. LV were also prepared in 2 or 4 mM Na_2HPO_4 solution.

2.3. Determination of turbidity kinetics upon adding electrolytes to DODAB BF

The turbidity of 0.5 mM DODAB BF at 300 nm as a function of time was recorded for 20 minutes after adding Na_2HPO_4, dAMP or poly (dA) over a range of low concentrations. Turbidity measurements were also obtained at 3 and 24 h of interaction between BF and electrolytes. All measurements were performed with 0.5 mM DODAB BF dispersion as a blank by means of a double-beam Hitachi U-2000 spectrophotometer.

2.4. Determination of size distribution, zeta-average diameter and zeta-potential for dispersions

Size distribution, zeta-average diameter and zeta-potential for dispersions were determined by dynamic light scattering using a Zeta-Plus Zeta-potential Analyzer (Brookhaven Instruments Corporation, Holtsville, NY) equipped with a 677 nm laser. The diameter referred to in this work from now on should be understood as the mean hydrodynamic (zeta-average) diameter Dz. Zeta-potentials (ζ) were determined from the electrophoretic mobility μ and Smoluchowski equation, $\zeta = \mu\eta/\varepsilon$, where η and ε are medium viscosity and dielectric constant, respectively. For zeta-potential and size distribution measurements, DODAB concentration was fixed at 0.5 mM and zeta-potential measurements were performed at and below the 2.5 mM Na_2HPO_4 limit of the Brookhaven apparatus. Dz and ζ represent mean values from at least 10 independent measurements performed 24 h of interaction between DODAB BF and electrolyte.

2.5. Determination of PyPC fluorescence spectra and PyPC excimer/monomer ratio

PyPC-labeled DODAB BF were prepared as follows. A 0.5 mL of a 10 mM chloroformic solution of DODAB containing 7 mol % of the fluorescent probe PyPC was evaporated under a nitrogen stream to form a film on the bottom of the sonication tube. The film was dried for 2 h in vacuum and then 25 mL of water solution was added to yield a final lipid concentration of 0.2 mM. Thereafter, 20 pulses of ultrasound of 1 minute each intercalated by 1 minute rest were used to disperse the film.

PyPC-labeled DODAB BF at 0.2 mM final lipid concentration were mixed with a stock DODAB BF dispersion at 2 mM and the volume completed to 100 μL with the desired electrolyte solution to yield a lipid concentration of 0.5 mM and a final 1:10 labeled/unlabeled BF proportion. After 20 minutes interaction, aliquots of 50 μL of the mixture were diluted to 0.5 mL to yield a final lipid concentration of 0.050 mM. The dilution served both to stop the interaction between fragments and to eliminate possible scattering artifacts. Fluorescence spectra were recorded at 30 °C using a Hitachi F-4500 Fluorescence Spectrophotometer at 344 nm as the excitation wavelength. Excitation and emission slits were 10 and 5 nm, respectively. The excimer/monomer (E/M) ratio was measured as the ratio of uncorrected fluorescence intensities at 470 and 395 nm. Appropriate controls were performed in order to confirm absence of spontaneous PyPC exchange between labeled and unlabeled DODAB BF.

2.6. Differential scanning calorimetry (DSC)

DODAB BF dispersions and electrolytes interacted for 24 h at 2 mM DODAB before performing DSC scans in a Microcal VP-DSC Microcalorimeter (Microcal Inc., Northampton, MA, USA) equipped with 0.5 mL twin total-fill cells. Heating rates were 20 °C/h. Scans were performed at least in duplicate. Tm was considered as the temperature of the most intense endothermic peak. The enthalpy of transition ΔH was obtained by integrating the area under the thermograms.

3. Results

3.1. Oligonucleotide and salt induced DSC scans for BF similar to the ones for LV

The bilayer structure of DODAB bilayer fragments (BF) in the presence of Na_2HPO_4, dAMP or poly (dA) was investigated by means of differential scanning calorimetry (DSC).

The gel-to-liquid-crystalline phase transition temperature (Tm) for DODAB large unilamellar vesicles (LV) at 44.7 °C was preceded by a less intense pre-transition at 36.1 °C (Fig. 1A), in good agreement with previous results from the literature [32–34]. The pre-transition has been attributed to a stretching of the alkyl chains with a loss of rotational disorder [34]. DODAB BF, on the other hand, presented a broader and less cooperative transition with the most intense peak at 43.7 °C (Fig. 1A). In the presence of salt (2 or 4 mM Na_2HPO_4), DSC scans for BF were similar to those obtained for LV (Fig. 1B, C and D). Mononucleotide dAMP barely changed the DSC scan recorded for BF (Fig. 2A and B), in contrast to the substantial modification induced by poly (dA) (Fig. 2C and D). At 0.04 mM poly (dA), besides the intense peak at 43.7 °C, there were two other peaks at 48 and 52 °C on the scan for BF (Fig. 2C). At 1 mM poly (dA), although the transition of DODAB BF remained broad, an additional and intense peak appeared at 53.4 °C (Fig. 2D).

Transition enthalpy values (ΔH) from analysis of DSC scans are in Table 1. They were 6.2 and 10.7 kcal/mol for DODAB BF and LV, respectively. Addition of Na_2HPO_4 or poly (dA) to BF increased ΔH to values similar to those of LV in water (Table 1). Addition of dAMP to BF did not change ΔH (Table 1).

3.2. Oligonucleotide or salt decreased colloid stability due to BF fusion

At 300 nm and 0.5 mM DODAB, BF turbidity increased with time after adding Na_2HPO_4 over a range of concentrations (0.5–2.5 mM)

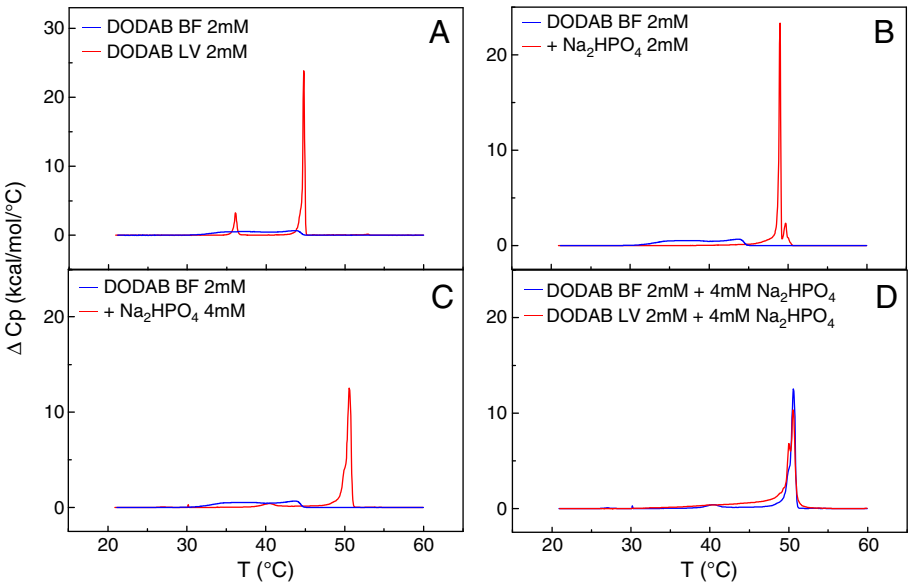

Fig. 1. Effect of Na_2HPO_4 on DSC thermograms of DODAB BF or LV (at 2 mM DODAB).

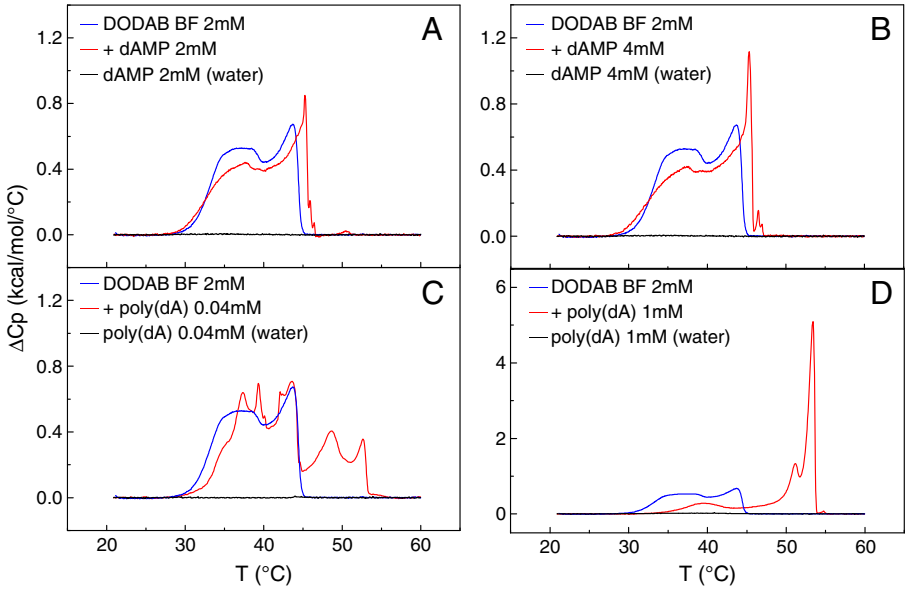

Fig. 2. Effect of dAMP (A and B) or poly (dA) (C and D) on DSC scans for DODAB BF (at 2 mM DODAB). Scans for dAMP or poly (dA) solutions in the absence of BF are also shown.

(Fig. 3A). In contrast, dAMP did not affect turbidity kinetics over the same range of concentrations (Fig. 3B). Poly (dA) over a range of concentrations (0.005–0.5 mM) affected turbidity kinetics in a nonmonotonic manner. Initial rate and maximal turbidity increased with poly (dA) concentration up to 0.05 mM. Above this concentration, they decreased with [poly (dA)] (Fig. 3C).

Effects of salt, dAMP or poly (dA) concentration on BF zeta-average diameter or zeta-potential are on Fig. 4. From 0 to 0.25 mM salt, Dz and zeta-potentials decreased with salt concentration possibly due to massive phosphate anion binding. From 0.25 to 2.5 mM salt, Dz increased but zeta-potential remained approximately constant and low (Fig. 4A and D).

Dz and zeta-potential decreased with dAMP concentration (0–2.5 mM) (Fig. 4B and E). At 0.05 mM poly (dA) and 0.5 mM DODAB, extensive BF aggregation and/or fusion took place as depicted from large Dz (>500 nm) (Fig. 4C) and zero of zeta-potential (Fig. 4F). Thus,

Table 1
Effect of Na_2HPO_4, dAMP or poly (dA) on main phase transition temperature (Tm) and transition enthalpy (ΔH) of DODAB BF in aqueous solutions of electrolytes at 2 mM DODAB.

DODAB dispersion	Electrolyte type	Electrolyte concentration (mM)	Temperature range for ΔH calculation (°C)	Tm ± s.d. (°C)	ΔH ± s.d. (kcal/mol)
LV	–	–	42–45	44.7 ± 0.1	10.7 ± 0.5
LV	Na_2HPO_4	4.00	30–55	50.5 ± 0.1	18.0 ± 0.2
BF	–	–	30–45	43.7 ± 0.1	6.2 ± 0.1
BF	Na_2HPO_4	2.00	40–55	48.9 ± 0.1	10.3 ± 0.1
BF	Na_2HPO_4	4.00	35–55	50.7 ± 0.1	12.1 ± 0.5
BF	dAMP	2.00	30–47	45.3 ± 0.1	6.1 ± 0.1
BF	dAMP	4.00	30–47	45.3 ± 0.1	6.5 ± 0.2
BF	poly (dA)	0.04	30–55	43.6 ± 0.1	7.9 ± 0.1
BF	poly (dA)	1.00	35–55	53.4 ± 0.2	10.7 ± 0.3

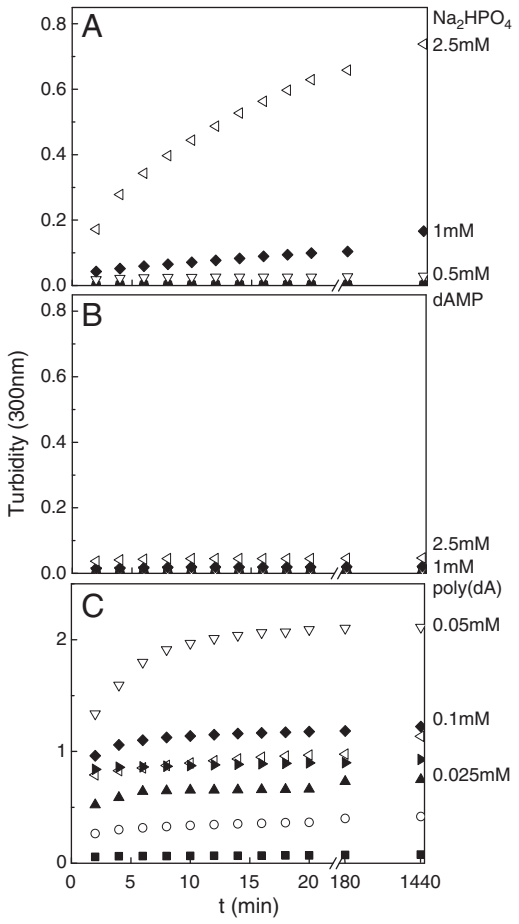

Fig. 3. Turbidity kinetics of DODAB BF at 300 nm after adding Na_2HPO_4 (A), dAMP (B) or poly (dA) over a range of concentrations (C). Final DODAB concentration was 0.5 mM. Na_2HPO_4 or dAMP final concentrations were 0.05 (■), 0.1 (○), 0.25 (▲), 0.5 (▽), 1 (♦) and 2.5 mM (◁). Poly (dA) concentrations were 0.005 (■), 0.01 (○), 0.025 (▲), 0.05 (▽), 0.1 (♦), 0.25 (◁) and 0.5 mM (►). Blank was DODAB BF at 0.5 mM DODAB.

charge neutralization took place at a 1: 10 poly (dA):DODAB molar ratio. Above 0.05 mM poly (dA), BF/poly (dA) assemblies were negatively charged (Fig. 4F) and Dz doubled in comparison to the one of BF in pure water (Fig. 4C). Similar behavior was reported for the interaction between other polyelectrolytes and oppositely charged liposomes [35,36] or particles [37,38].

The decrease of PyPC excimer to monomer ratio (E/M) has often been employed to characterize bilayer fusion of lecithin, DODAB or mitochondrial mimetic vesicles [39–41]. Fusion of PyPC-labeled and unlabeled BF would dilute the probe within the bilayer phase thereby decreasing E/M [39]. Fig. 5 shows the effect of [Na_2HPO_4], [dAMP] and [poly (dA)] on E/M determined for BF after 20 minutes of interaction time with each electrolyte concentration. Appropriate controls were performed to establish that E/M remained constant with time in absence of the electrolytes. E/M decreased as a function of [Na_2HPO_4] (Fig. 5A and B) or [poly (dA)] (Fig. 5E and F) but remained constant as a function of [dAMP] (Fig. 5C and D). In particular, the E/M decrease to 0.4 from 0.005 mM poly (dA), suggested extensive BF fusion induced by the oligonucleotide.

4. Discussion

The ΔH for fragments is about 50% of the one for vesicles (Table 1), in agreement with previous observations [42]. Low cooperativity during the phase transition from broad DSC profiles and small transition enthalpies can be explained by a looser lipid packing at the hydrophobic edges of DODAB BF in contrast to the tighter one in BF center, where lipids are in the gel phase [12]. In fact, approaches based on ESR and NMR have shown that there is a coexistence of the two phases in DODAB BF and only 50% of DODAB BF lipids are in the gel phase [9,43].

In the presence of Na_2HPO_4, the transition profile and ΔH value for DODAB BF became similar to the ones observed for DODAB LV in water (Fig. 1A, B and C; Table 1), suggesting fusion and increase in bilayer packing due to screening of the bilayer charges by salt. In fact, another independent set of data represented by E/M decrease as a function of salt concentration demonstrated Na_2HPO_4-induced fusion of BF (Fig. 5B).

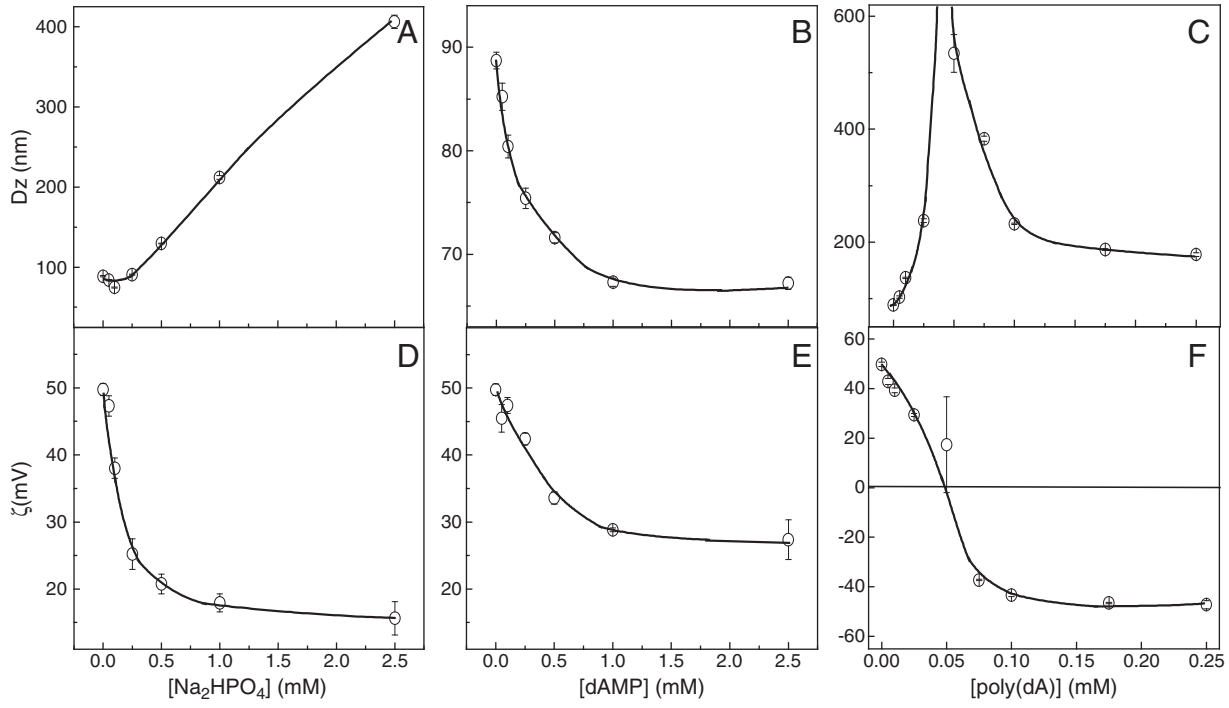

Fig. 4. Effect of Na_2HPO_4, dAMP or poly (dA) concentration on the zeta-average diameter (A, B and C) and zeta-potential of DODAB BF at 0.5 mM DODAB (D, E and F).

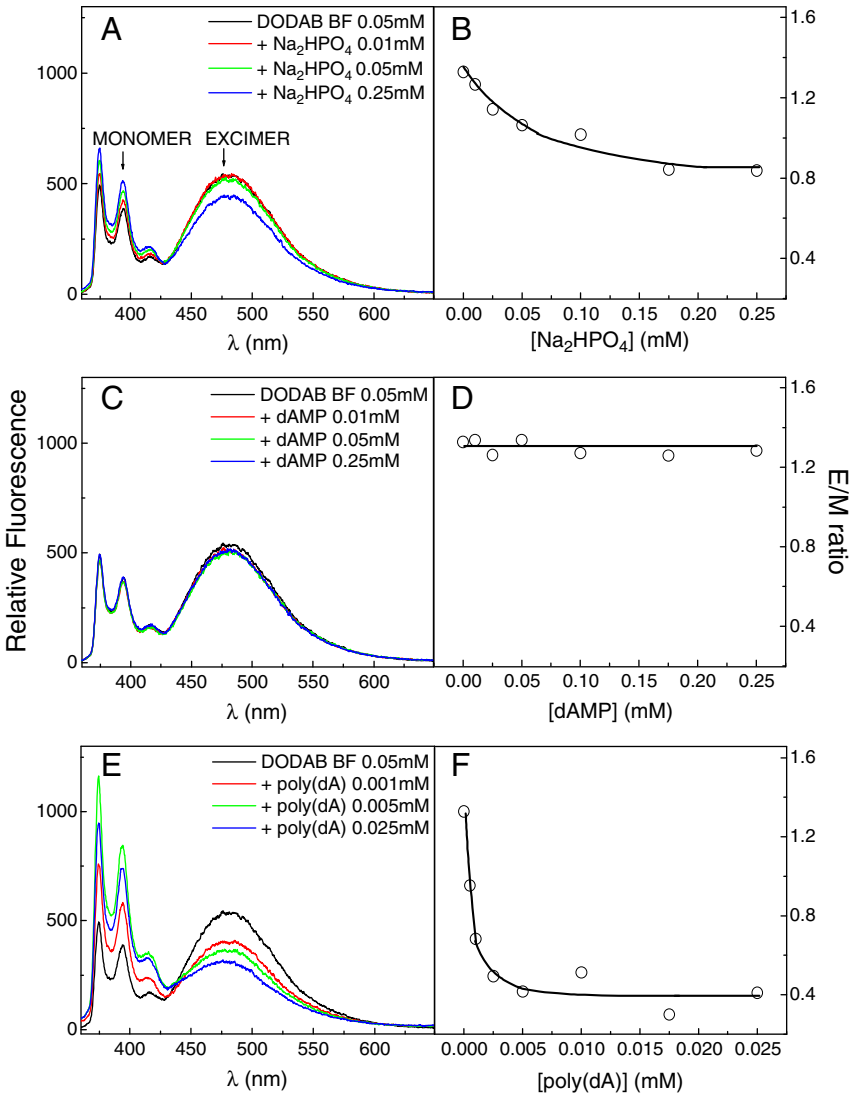

Fig. 5. Effect of Na_2HPO_4 (A), dAMP (C) or poly (dA) concentration on fluorescence spectra of PyPC in DODAB BF (E) or on the excimer to monomer (E/M) ratio (B, D and F). Excitation wavelength was 344 nm. Final DODAB concentration was 0.05 mM. Labeled DODAB BF contained 7 mol % PyPC. Labeled and unlabeled DODAB BF at 1:10 vol./vol. interacted for 20 minutes before 1:10 dilution for recording the PyPC fluorescence spectra.

There was a large difference in the behavior of the bilayer structure in the presence of dAMP or divalent salt. While dAMP did not affect ΔH for the bilayer transition, a large effect on ΔH was observed due to divalent salt (Table 1). Possibly this was due to the more efficient screening by the divalent counterion binding in comparison to the one by the bulky mononucleotide. Accordingly, the zeta-potential at equivalent amount of charge was 20 and 30 mV at 1 mM Na_2HPO_4 and 2 mM dAMP, respectively (Fig. 4D and E). Furthermore, the divalent anion induced fusion whereas dAMP not only did not induce fusion but also caused a slight decrease in Dz and did not affect turbidity values (Figs. 3B, 4B and 5D). Circular dichroism spectra and molecular dynamics simulations for DODAB/dAMP assemblies have previously shown that DODAB BF changed dAMP conformation from *anti* to *syn* approaching the nucleotide sugar moiety of the bilayer-water interface [44]. Thereby, bulky dAMP would not be able to neutralize completely all positive charges on the bilayer. The conformation adopted by dAMP while interacting with DODAB bilayers would limit further dAMP adsorption onto the bilayer [45]. In fact, LV electrophoretic mobility was minimal and positive from 2:1 dAMP:DODAB molar ratio [45]. Consistently, BF zeta-potential was minimal and positive from 4:1 dAMP:DODAB molar ratio (Fig. 4E). LV adsorbed dAMP only at its outer monolayer in contrast to BF that exposed both monolayers to interact with dAMP.

At 1 mM poly (dA), the intense endothermic peak in DSC scan for BF appearing above 50 °C (Fig. 2D) was previously described for DODAB vesicles interacting with double-stranded DNA [46]. Since single-stranded oligonucleotides with less than 20 nucleotide residues were shown to behave as rigid charged rods in solution [47], poly (dA) would adsorb on the positively charged DODAB bilayer without formation of trains and loops. The electrostatic interaction between phosphate on poly (dA) backbone and cationic polar heads of BF might have increased molecular packing at the BF bilayer level so that the ΔH value increased to a value similar to the one of DODAB LV in pure water (Table 1). The experiments for detecting BF fusion induced by the oligonucleotide showing E/M decrease for BF interacting with poly (dA) (Fig. 5F) further supported the conversion of BF onto more extensive and tightly packed bilayer areas suggesting BF fusion.

The onset of poly (dA) induced fusion could be consistently observed by three different techniques such as significant turbidity kinetics at 300 nm from 0.01 mM poly (dA) at 0.5 mM DODAB (Fig. 3C), E/M decrease from 0.001 mM poly (dA) and 0.050 mM DODAB (Fig. 5F) and appearance of additional endothermic peaks around 50 °C on the DSC

scans from 0.04 mM poly(dA) and 2.0 mM DODAB (Fig. 2C). The molar ratio poly (dA):DODAB was 1:50 by the three techniques employed. At the molar proportion of 1:2 poly (dA):DODAB, E/M ratio is at its minimum (Fig. 5F), fusion is at its maximum and the phase transition presents an intense peak at 53.4 °C and a ΔH value similar to the one of DODAB LV in pure water (Fig. 2D; Table 1), confirming that poly (dA)-induced fragments fusion led to formation of extensive bilayer areas.

The turbidity increase at and above the 1:1 Na_2HPO_4:DODAB molar ratio (Fig. 3A) was consistent with the increase in size (Fig. 4A). Concomitantly, the zeta-potential decreased steeply with addition of Na_2HPO_4 and reached a plateau from the 1:1 Na_2HPO_4:DODAB molar ratio (Fig. 4D). The screening of DODAB charges by Na_2HPO_4 would mean a decrease in electrostatic repulsion between fragments contributing to destabilization and fusion of DODAB BF. Over the same range of concentrations, dAMP did not affect turbidity of DODAB BF (Fig. 3B) or did not cause fragments fusion due to its bulky nature (Fig. 5C and D).

The explanation for the dAMP-induced decrease in Dz of DODAB BF (Fig. 4B) can simply be related to electrostatics and colloid stability modulated by improved hydration at the bilayer surface given the proximity of the deoxyribose moiety of dAMP. In fact, hydrated counterions bound to the bilayer surface were also the most reasonable explanation for the decrease in size below the 1:1 Na_2HPO_4:DODAB molar ratio (Fig. 4A) as previously reported for similar systems [48,49]. Binding of hydrated counterions have been implicated in hydration repulsion and colloid stabilization accounting for the large decrease in zeta-potential (Fig. 4D). The conformation adopted by dAMP while interacting with DODAB bilayers would limit its adsorption to the bilayer [45] explaining why the plateau reached above the 1:1 dAMP: DODAB molar ratio that takes place at potentials about 10 mV higher than the ones observed for Na_2HPO_4 (Fig. 4E). It is more difficult for dAMP to reduce the bilayer charge than it is for Na_2HPO_4 under conditions of equivalence of total negative charge. This highlights the importance of anion nature on the interaction with the cationic bilayer.

The nonmonotonic effect of poly (dA) concentration on turbidity kinetics and zeta-average diameter represented by increase up to 0.05 mM oligonucleotide and decrease above this value (Figs. 3C and 4C) is typical of polyelectrolytes interacting with particles of opposite charge [35,36,49]. Charge neutralization led to flocculation and charge overcompensation led to colloidal restabilization due to recovery of the electrostatic repulsion between the assemblies, in contrast to the monotonic effects of equivalent Na_2HPO_4 or dAMP concentrations (Figs. 3A and B, 4A and B). Over the region of charge overcompensation, sizes practically doubled (Fig. 4C) as also observed for long and single-stranded DNA molecules interacting with liquid-crystalline DOTAP vesicles [50]. Transmission electron microscopy images suggested vesicle aggregation rather than fusion [50]. On the other hand, the interaction between a cationic polymer and small anionic vesicles in the gel state led to fusion [36,51], in agreement with the extensive DODAB BF fusion induced by poly (dA) (Fig. 5F). The quickest and most extensive flocculation kinetics induced by poly (dA) occurred at a molar ratio of 1:10 poly (dA):DODAB (Figs. 3C and 4C). At this experimental condition, one molecule of poly (dA) is adsorbed to 10 DODAB molecules. Since each poly (dA) molecule bears 10 negatively charged phosphates in its backbone, it should be able to neutralize 10 DODAB molecules at the bilayer surface, as indeed observed. This molar ratio at the point of zero charge would be consistent with a bilayer fragment structure in which both monolayers are exposed to the medium [7] rather than with a structure of small prolate vesicles [42]. For closed bilayers, the molar proportion at charge neutralization would be 1:20 poly (dA):DODAB since only DODAB molecules of the outer monolayer would be available to adsorb poly (dA).

5. Conclusions

Over a range of equivalent concentrations, oligonucleotide and salt increased bilayer packing due to BF fusion. Mononucleotide did not reduce colloid stability nor caused BF fusion. Charge neutralization of BF by poly (dA) caused extensive aggregation and maximal size for DODAB BF/poly (dA) assemblies. Above charge neutralization, assemblies recovered stability due to charge overcompensation. The nonmonotonic effect of poly (dA) concentration on colloid stability was not observed for Na_2HPO_4 or dAMP. For the first time, such interactions between cationic bilayer fragments and mono- or oligonucleotide were described in the literature. BF/oligonucleotide assemblies may find interesting applications in drug delivery.

Acknowledgements

Financial support from FAPESP and CNPq is gratefully acknowledged. J.H.K.R. thanks CNPq for a PhD fellowship. We thank Prof Frank Quina for the use of Hitachi F-4500 Fluorescence Spectrophotometer.

References

[1] A.M. Carmona-Ribeiro, Synthetic amphiphile vesicles, Chem. Soc. Rev. 21 (1992) 209–214.
[2] A.M. Carmona-Ribeiro, Bilayer-forming synthetic lipids: drugs or carriers? Curr. Med. Chem. 10 (2003) 2425–2446.
[3] A.M. Carmona-Ribeiro, H. Chaimovich, Preparation and characterization of large dioctadecyldimethylammonium chloride liposomes and comparison with small sonicated vesicles, Biochim. Biophys. Acta 733 (1983) 172–179.
[4] A.M. Carmona-Ribeiro, C.E. Castuma, A. Sesso, S. Schreier, Bilayer structure and stability in dihexadecyl phosphate dispersions, J. Phys. Chem. 95 (1991) 5361–5366.
[5] M. Andersson, L. Hammarström, K. Edwards, Effect of bilayer phase transitions on vesicle structure and its influence on the kinetics of viologen reduction, J. Phys. Chem. 99 (1995) 14531–15538.
[6] L. Hammarström, I. Velikian, G. Karlsson, K. Edwards, Cryo-TEM evidence: sonication of dihexadecyl phosphate does not produce closed bilayer with smooth curvature, Langmuir 11 (1995) 408–410.
[7] R.B. Pansu, B. Arrio, J. Roncin, J. Faure, Vesicles versus membrane fragments in DODAC suspensions, J. Phys. Chem. 94 (1990) 796–801.
[8] E. Feitosa, W. Brown, Fragment and vesicle structures in sonicated dispersions of dioctadecyldimethylammonium bromide, Langmuir 13 (1997) 4810–4816.
[9] C.R. Benatti, E. Feitosa, R.M. Fernandez, M.T. Lamy-Freund, Structural and thermal characterization of dioctadecyldimethylammonium bromide dispersions by spin labels, Chem. Phys. Lipids 111 (2001) 93–104.
[10] D.B. Vieira, A.M. Carmona-Ribeiro, Synthetic bilayer fragments for solubilization of amphotericin B, J. Colloid Interface Sci. 244 (2001) 427–431.
[11] L.F. Pacheco, A.M. Carmona-Ribeiro, Effects of synthetic lipids on solubilization and colloid stability of hydrophobic drugs, J. Colloid Interface Sci. 258 (2003) 146–154.
[12] D.B. Vieira, L.F. Pacheco, A.M. Carmona-Ribeiro, Assembly of a model hydrophobic drug into cationic bilayer fragments, J. Colloid Interface Sci. 293 (2006) 240–247.
[13] S.P. Moura, A.M. Carmona-Ribeiro, Cationic bilayer fragments on silica at low ionic strength: competitive adsorption and colloid stability, Langmuir 19 (2003) 6664–6667.
[14] H. Rosa, D.F.S. Petri, A.M. Carmona-Ribeiro, Interactions between bacteriophage DNA and cationic biomimetic particles, J. Phys. Chem. B 112 (2008) 16422–16430.
[15] N. Lincopan, N.M. Espíndola, A.J. Vaz, A.M. Carmona-Ribeiro, Cationic supported lipid bilayers for antigen presentation, Int. J. Pharm. 340 (2007) 216–222.
[16] N. Lincopan, N.M. Espíndola, A.J. Vaz, M.H.B. da Costa, E. Faquim-Mauro, A.M. Carmona-Ribeiro, Novel immunoadjuvants based on cationic lipid: preparation, characterization and activity in vivo, Vaccine 27 (2009) 5760–5771.
[17] S. Weisman, D. Hirsch-Lerner, Y. Barenholz, Y. Talmon, Nanostructure of cationic lipid–oligonucleotide complexes, Biophys. J. 87 (2004) 609–614.
[18] P.C. Zamecnik, M.L. Stephenson, Inhibition of Rous sarcoma virus replication and cell transformation by a specific oligodeoxynucleotide, Proc. Natl Acad. Sci. USA 75 (1978) 280–284.
[19] K.T. Flaherty, J.P. Stevenson, P.J. O'Dwyer, Antisense therapeutics: lessons from early clinical trials, Curr. Opin. Oncol. 13 (2001) 499–505.
[20] I. Tamm, B. Dörken, G. Hartmann, Antisense therapy in oncology: new hope for an old idea? Lancet 358 (2001) 489–497.
[21] M.D. De-Backer, B. Nelissen, M. Logghe, J. Viaene, I. Loonen, S. Vandoninck, R. de-Hoogt, S. Dewaele, F.A. Simons, P. Verhasselt, G. Vanhoof, R. Contreras, W.H. Luyten, An antisense-based functional genomics approach for identification of genes critical for growth of *Candida albicans*, Nat. Biotechnol. 19 (2001) 235–241.
[22] N.M. Dean, Functional genomics and target validation approaches using antisense oligonucleotide technology, Curr. Opin. Biotechnol. 12 (2001) 622–625.
[23] R. Juliano, M.R. Alam, V. Dixit, H. Kang, Mechanisms and strategies for effective delivery of antisense and siRNA oligonucleotides, Nucleic Acids Res. 36 (2008) 4158–4171.
[24] L. Liu, X. Zhou, H. Liu, L. Xiang, Z. Yuan, CpG motif acts as a danger signal and provides a T helper type 1-biased microenvironment for DNA vaccination, Immunology 115 (2005) 223–230.
[25] D.E. Fonseca, J.N. Kline, Use of CpG oligonucleotides in treatment of asthma and allergic disease, Adv. Drug Deliv. Rev. 61 (2009) 256–262.
[26] Y. Kuramoto, M. Nishikawa, K. Hyoudou, F. Yamashita, M. Hashida, Inhibition of peritoneal dissemination of tumor cells by single dosing of phosphodiester

CpG oligonucleotide/cationic liposome complex, J. Control. Release 115 (2006) 226–233.
[27] F. Shi, D. Hoekstra, Effective intracellular delivery of oligonucleotides in order to make sense of antisense, J. Control. Release 97 (2004) 189–209.
[28] P.L. Felgner, T.R. Gadek, M. Holm, R. Roman, H.W. Chan, M. Wenz, J.P. Northrop, G.M. Ringold, M. Danielsen, Lipofection: a highly efficient, lipid-mediated DNA-transfection procedure, Proc. Natl Acad. Sci. USA 84 (1987) 7413–7417.
[29] J.H. Fendler, Surfactant vesicles as membrane mimetic agents: characterization and utilization, Acc. Chem. Res. 13 (1980) 7–13.
[30] O. Schales, S. Schales, A simple and accurate method for the determination of chloride in biological fluids, J. Biol. Chem. 140 (1941) 879–884.
[31] D. Katz, C.A. Kraaijeveld, H. Snippe, Synthetic lipoid compounds as antigen-specific immunostimulators for improving the efficacy of killed-virus vaccines, in: D.E.S. Stewart-Tull (Ed.), The theory and practical application of adjuvants, John Wiley & Sons, Chichester, 1995, pp. 37–50.
[32] D.B. Nascimento, R. Rapuano, M.M. Lessa, A.M. Carmona-Ribeiro, Counterion effects on properties of cationic vesicles, Langmuir 14 (1998) 7387–7391.
[33] E. Feitosa, P.C.A. Barreleiro, G. Olofsson, Phase transition in dioctadecyldimethylammonium bromide and chloride vesicles prepared by different methods, Chem. Phys. Lipids 105 (2000) 201–213.
[34] P. Saveyn, P. Van der Meeren, M. Zackrisson, T. Narayanan, U. Olsson, Subgel transition in diluted vesicular DODAB dispersions, Soft Matter 5 (2009) 1735–1742.
[35] A.V. Sybachin, A.A. Efimova, E.A. Litmanovich, F.M. Menger, A.A. Yaroslavov, Complexation of polycations to anionic liposomes: composition and structure of the interfacial complexes, Langmuir 23 (2007) 10034–10039.
[36] A.A. Yaroslavov, A.A. Rakhnyanskaya, E.G. Yaroslavova, A.A. Efimova, F.M. Menger, Polyelectrolyte-coated liposomes: stabilization of the interfacial complexes, Adv. Colloid Interface Sci. 142 (2008) 43–52.
[37] F.M. Correia, D.F.S. Petri, A.M. Carmona-Ribeiro, Colloid stability of lipid/polyelectrolyte decorated latex, Langmuir 20 (2004) 9535–9540.
[38] F.P. Araujo, D.F.S. Petri, A.M. Carmona-Ribeiro, Colloid stability of sodium dihexadecyl phosphate/poly (diallyldimethylammonium chloride) decorated latex, Langmuir 21 (2005) 9495–9501.
[39] S. Schenkman, P.S. Araujo, R. Dijkman, F.H. Quina, H. Chaimovich, Effects of temperature and lipid composition on the serum albumin-induced aggregation and fusion of small unilamellar vesicles, Biochim. Biophys. Acta 649 (1981) 633–641.
[40] A.M. Carmona-Ribeiro, L.S. Yoshida, H. Chaimovich, Salt effects on the stability of dioctadecyldimethylammonium chloride and sodium dihexadecyl phosphate vesicles, J. Phys. Chem. 89 (1985) 2928–2933.
[41] J.M. Holopainen, J.Y.A. Lehtonen, P.K.J. Kinnunen, Evidence for the extended phospholipid conformation in membrane fusion and hemifusion, Biophys. J. 76 (1999) 2111–2120.
[42] P. Saveyn, P. Van der Meeren, J. Cocquyt, T. Drakenberg, G. Olofsson, U. Olsson, Incomplete lipid chain freezing of sonicated vesicular dispersions of double-tailed ionic surfactants, Langmuir 23 (2007) 10455–10462.
[43] J. Cocquyt, U. Olsson, G. Olofsson, P. Van der Meeren, Temperature quenched DODAB dispersions: fluid and solid state coexistence and complex formation with oppositely charged surfactant, Langmuir 20 (2004) 3906–3912.
[44] I.L. Nantes, F.M. Correia, A. Faljoni-Alario, A.E. Kawanami, H.M. Ishiki, A.T. Amaral, A.M. Carmona-Ribeiro, Nucleotide conformational change induced by cationic bilayers, Arch. Biochem. Biophys. 416 (2003) 25–30.
[45] I.S. Kikuchi, W. Viviani, A.M. Carmona-Ribeiro, Nucleotide insertion in cationic bilayers, J. Phys. Chem. 103 (1999) 8050–8055.
[46] P.C.A. Barreleiro, G. Olofsson, P. Alexandridis, Interaction of DNA with cationic vesicles: a calorimetric study, J. Phys. Chem. B 104 (2000) 7795–7802.
[47] H.W. Walker, S.B. Grant, Influence of surface charge and particle size on the stabilization of colloidal particles by model polylectrolytes, Colloids Surf. A 135 (1998) 123–133.
[48] A.M. Carmona-Ribeiro, B.R. Midmore, Surface potential in charged synthetic amphiphile vesicles, J. Phys. Chem. 96 (1992) 3542–3547.
[49] V.A. Kabanov, A.A. Yaroslavov, What happens to negatively charged lipid vesicles upon interacting with polycation species? J. Control. Release 78 (2002) 267–271.
[50] S. Sennato, F. Bordi, C. Cametti, M. Diociaiuti, P. Malaspina, Charge patch attraction and reentrant condensation in DNA–liposome complexes, Biochim. Biophys. Acta 1714 (2005) 11–24.
[51] A.A. Yaroslavov, A.A. Efimova, V.I. Lobyshev, V.A. Kabanov, Reversibility of structural rearrangements in the negative vesicular membrane upon electrostatic adsorption/desorption of the polycation, Biochim. Biophys. Acta 1560 (2002) 14–24.